

## Electronic Supplementary Information

### Photocatalytic ethene synthesis from ethane dehydrogenation with high selectivity by ZnO-supported Pt nanoparticles

Wenyu Guo,<sup>a</sup> Wenwen Shi,<sup>a</sup> Junjian Cai,<sup>a</sup> Fen Wei,<sup>a</sup> Xiahui Lin,<sup>\*,b</sup> Xuefeng Lu,<sup>a</sup>  
Zhengxin Ding,<sup>\*,a</sup> Yidong Hou,<sup>a</sup> Guigang Zhang<sup>a</sup> and Sibowang<sup>\*,a</sup>

<sup>a</sup>State Key Laboratory of Photocatalysis on Energy and Environment, College of  
Chemistry, Fuzhou University, Fuzhou 350116, P. R. China

E-mail: [zxding@fzu.edu.cn](mailto:zxding@fzu.edu.cn); [sibowang@fzu.edu.cn](mailto:sibowang@fzu.edu.cn)

<sup>b</sup>College of Environment and Safety Engineering, Fuzhou University, Fuzhou, 350108,  
China

E-mail: [linxiahui@fzu.edu.cn](mailto:linxiahui@fzu.edu.cn)

## Experimental details

**Materials characterization.** Powder X-ray diffraction (XRD) tests were carried out on a Rigaku Miniflex 600 Advance X-ray instrument (Cu  $K_{\alpha 1}$  radiation,  $\lambda = 1.5406 \text{ \AA}$ ) at a voltage of 40 kV and a current of 40 mA. Zeta potential analysis was performed on a ZS90 (Malvern) instrument. Double beam field-emission scanning electron microscope (FESEM; Thermo Scientific, Helios G4 CX) and transmission electron microscope (TEM; Philips, Tecnai 20 FEI) were used to examine the morphology and structure of the samples. The compositions of the samples were determined by energy-dispersive X-ray spectroscopy (EDS) attached to Field-emission scanning electron microscope (HITACHI SU-8010) and inductively coupled plasma optical emission spectrometer (ICP-OES; Perkin Elmer, Avio 200). X-ray photoelectron spectroscopy (XPS) analysis and Ultraviolet photoelectron spectra were carried out on a ESCALAB Xi250 (Thermo Scientific) XPS system with C 1s binding energy (284.8 eV) as the reference and He I excitation (21.22 eV) as the monochromatic light source.  $N_2$  adsorption-desorption isotherms characterizations were conducted on a Micromeritics ASAP2020 under liquid nitrogen (77K) temperature. Thermogravimetric analyses (TGA) were carried out in air atmosphere from 20 to 800 °C with a ramp of 10 °C  $\text{min}^{-1}$  using a NETZSCH STA 449 F3 Jupiter. UV-vis-NIR diffuse reflectance spectra (DRS) were obtained on an Agilent Cary 5000 UV-vis spectrometer equipped with an integrating sphere using  $\text{BaSO}_4$  as the reference. A QP2020N gas chromatography mass spectrometry (GC-MS) was used to detect product generated from the isotope experiment. The room temperature photoluminescence (PL) characterizations were carried out on Hitachi F-7000 spectrophotometer. The fluorescence lifetime is determined by recording the time-resolved fluorescence emission spectra on a Deltapro Fluorescence Lifetime System. The electrochemical analysis was carried out on a SP-200 (Bio-Logic) electrochemical workstation, using the conventional three electrodes cell with Pt and Ag/AgCl as the counter electrode and reference electrode, respectively. Typically, 10 mg of the samples were dispersed in the mixed solution of DMF (1mL) and Nafion (0.1 mL) by sonication to gain a suspension. Then, the resultant slurry was spread onto the

FTO glass with an area of *ca.* 0.25 cm<sup>2</sup>. The transient photocurrent response spectra were collected in Na<sub>2</sub>SO<sub>4</sub> aqueous solution (0.2 M) with a 300 W xenon lamp as a light source. Electrochemical impedance spectroscopy (EIS) measurements were carried out at the open circuit potential in [Fe(CN)<sub>6</sub>]<sup>3+</sup>/[Fe(CN)<sub>6</sub>]<sup>2+</sup> aqueous solution.

**C<sub>2</sub>H<sub>4</sub>-TPD and H<sub>2</sub>-TPD tests.** 50 mg sample was placed in the middle of the quartz glass tube and fixed with quartz cotton on both sides. The quartz tube was then placed into a high-temperature furnace. Then, the system was changed to the N<sub>2</sub> purification mode and pre-treated at 150 °C for 60 min at a heating rate of 10 °C min<sup>-1</sup> to remove the impurities adsorbed on the catalyst surface. After heat preservation, it naturally cooled down to room temperature. Then, 10% C<sub>2</sub>H<sub>4</sub>/N<sub>2</sub> mixture was injected and adsorbed for 1 h. After adsorption, N<sub>2</sub> was introduced, and a TCD current of 100 mA was applied with a TCD temperature of 80 °C, allowing for a baseline equilibrium of 30 min. After the baseline was stabilized, temperature was programmed (the temperature was increased to 850 °C at a heating rate of 10 °C min<sup>-1</sup> under normal N<sub>2</sub> atmosphere). After the test was finished, the signals from the heating section were taken for plotting. The test of H<sub>2</sub>-TPD is the same as the above procedure, except that the 10% C<sub>2</sub>H<sub>4</sub>/N<sub>2</sub> mixture gas is changed to 5% H<sub>2</sub>/N<sub>2</sub> mixture.

**CO pulse titration test.** Conventional procedures for dispersion: 100 mg Pt/ZnO sample was first screened with a grain size of 60 mesh. To start the test, 10% H<sub>2</sub>/Ar mixture (pretreatment gas) was treated at 200 °C for 30 min, and then switched to He/Ar gas for purging to 50 °C. Pulse experiments were carried out under the pulse system, and the atomic weight of precious metals on the surface was calculated according to the adsorption capacity, and finally the metal dispersion was determined.

***In-situ* DRIFTS.** The *in-situ* DRIFTS measurements were carried out on a Nicolet IS50-FTIR spectrometer (Thermo Scientific) equipped with a MCT detector and a designed reaction cell. A thin layer of the sample was loaded on the substrate that is placed in the center of the reaction cell. Before conducting the adsorption measurements of C<sub>2</sub>H<sub>6</sub>, a flow of N<sub>2</sub> (20 mL min<sup>-1</sup>) was employed to purge the cell of any remaining

gases and remove adsorbed species from the catalyst surface. Subsequently, the flowing mixture of C<sub>2</sub>H<sub>6</sub> (20 mL min<sup>-1</sup>) and N<sub>2</sub> (20 mL min<sup>-1</sup>) were introduced while simultaneously initiating the recording of the adsorption curve of ethane over time at room temperature. After reaching saturation of C<sub>2</sub>H<sub>6</sub> adsorption, background subtraction was performed on the ethane adsorption curve, and baseline data were reacquired. Ultimately, the xenon lamp light source was turned on, and signals indicating intermediate changes during the reaction were recorded at regular intervals.

**Calculation of band structures from UPS spectrum.** The work function ( $\phi$ ) can be calculated by Eq. (1):  $\phi = h\nu - E_{\text{SEO}}$ . Here,  $h\nu$  (21.22 eV) represents the energy of monochromatic ionizing light, while  $E_{\text{SEO}}$  is the secondary electron onset obtained from the linear extrapolation of UPS spectrum.

The Fermi level ( $E_f$ ) is obtained from work function by Eq. (2):  $E_f = -\phi$ .

The valence band (VB) potential ( $E_{\text{VB}}$ ) is obtained by Eq. (3):  $E_{\text{VB}} = E_f - X$ , in which  $X$  is obtained from the extrapolation of onsets of UPS spectrum. Therefore, the conduction band (CB) potential ( $E_{\text{CB}}$ ) is obtained by Eq. (4):  $E_{\text{CB}} = E_{\text{VB}} + E_g = E_f - X + E_g$ . Here,  $E_g$  is the bandgap energy obtained by the Tauc plot.

All the potentials mentioned above refer to the vacuum energy. The vacuum energy ( $E_{\text{vac}}$ ) in electronvolt (eV) can be converted to  $E$  (V vs. RHE) according to the formula between the reversible hydrogen electrode (RHE) and  $E_{\text{vac}}$  (i.e.,  $E_{\text{RHE}} = -E_{\text{vac}} - 4.44$ ). The potential of RHE equals to the normal hydrogen electrode (NHE) at pH = 0. Based on the relationship between RHE and NHE (i.e.,  $E_{\text{NHE}} = E_{\text{RHE}} - 0.0591\text{pH}$ ), the potential can be converted to  $E$  (V vs. NHE, pH = 7).

The work function of ZnO was determined as 4.07 eV (vs.  $E_{\text{vac}}$ ), applying the method of linear approximation to the UPS spectrum to obtain the secondary electron onset (i.e., 17.15 eV vs.  $E_{\text{vac}}$ , Fig. 1c). The Fermi level of ZnO was estimated as -4.07 eV (vs.  $E_{\text{vac}}$ ). Simultaneously,  $E_{\text{VB}}$  of ZnO is calculated as -7.16 eV (vs.  $E_{\text{vac}}$ ). According to the formula  $E_{\text{RHE}} = -E_{\text{vac}} - 4.44$ ,  $E_{\text{VB}}$  of ZnO is determined as 2.72 V (vs. RHE), corresponding to 2.31 V (vs. NHE, pH = 7). Therefore, considering the bandgap energy of 3.2 eV,  $E_{\text{CB}}$  of ZnO is about -0.89 V (vs. NHE, pH = 7).

**The calculation details of turnover number (TON)** The calculation details of turnover number (TON) are as follows:

The mole of Pt sites is 2.966  $\mu\text{mol}$ , which is determined by ICP-OES (Table S1) and CO pulse analysis (Pt dispersion: 6.151%, Fig. S13). The accumulated evolution of  $\text{C}_2\text{H}_4$  in 8 h cyclic tests are *ca.* 6616.4  $\mu\text{mol}$  (Fig. 3b), corresponding to a turnover number (TON) of *ca.* 2231 based on the active Pt sites.

$$\text{TON} = \frac{\text{Mole of C}_2\text{H}_4 \text{ molecules evolved}}{\text{Mole of Pt sites}} = \frac{6616.4 \mu\text{mol}}{2.966 \mu\text{mol}} = 2231$$

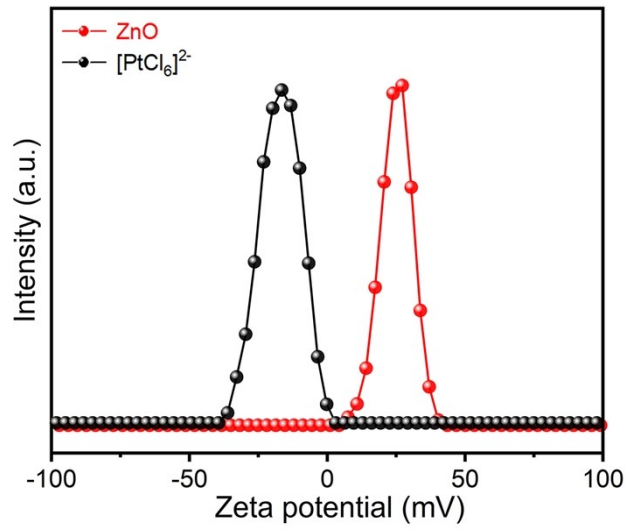


**Fig. S1** Zeta potentials of ZnO and  $\text{H}_2\text{PtCl}_6$  dispersed in  $\text{H}_2\text{O}$ .

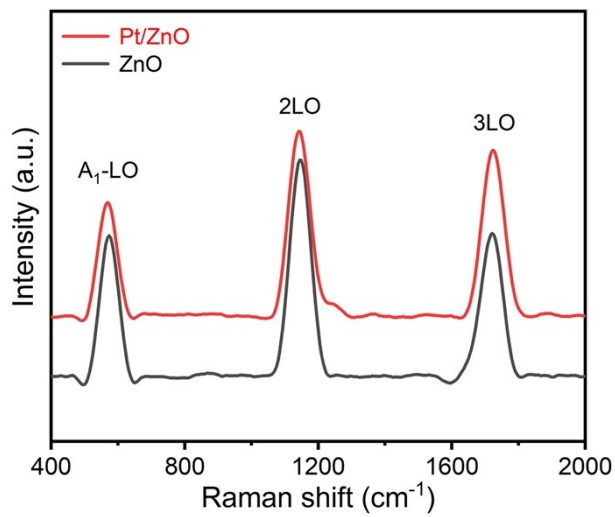


**Fig. S2** Raman spectra of ZnO and Pt/ZnO.

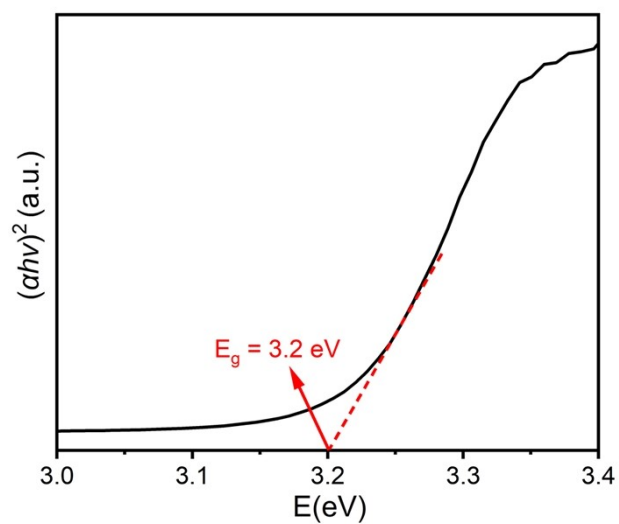


**Fig. S3** Tauc plot of ZnO.

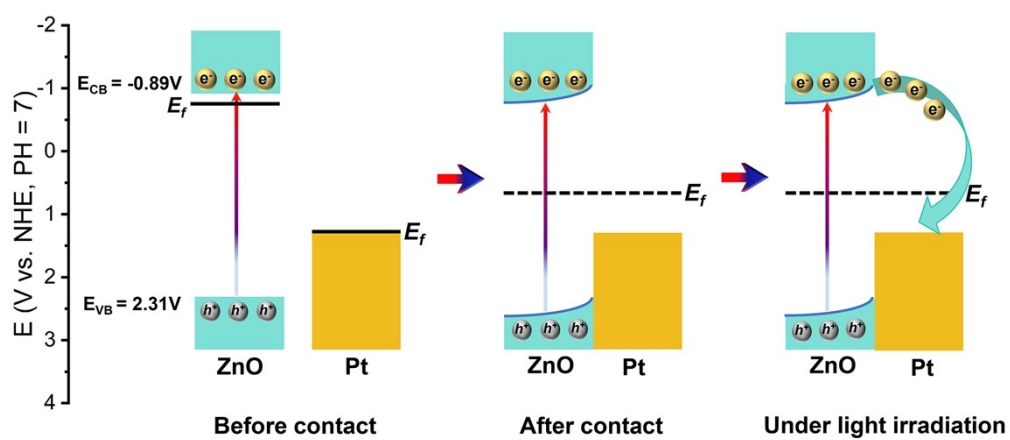


**Fig. S4** Schematic illustration of band diagram for Pt/ZnO.

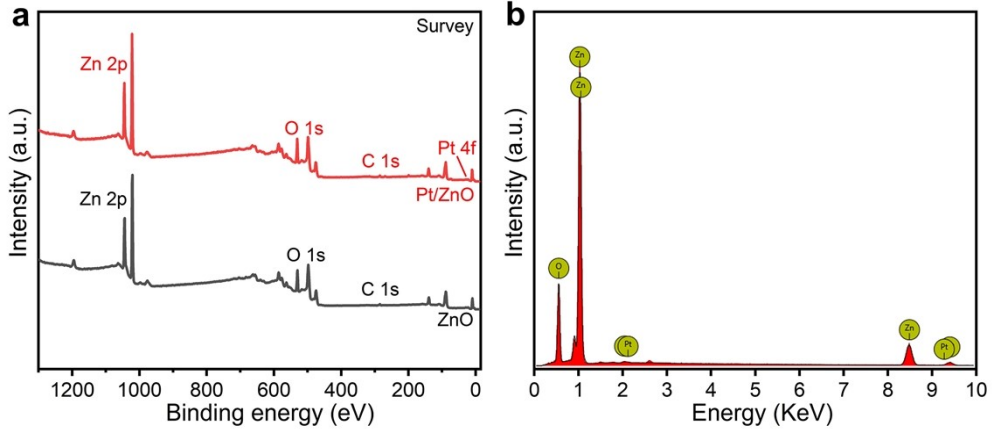


**Fig. S5** (a) XPS survey spectra of ZnO and Pt/ZnO and (b) EDS spectrum of Pt/ZnO.

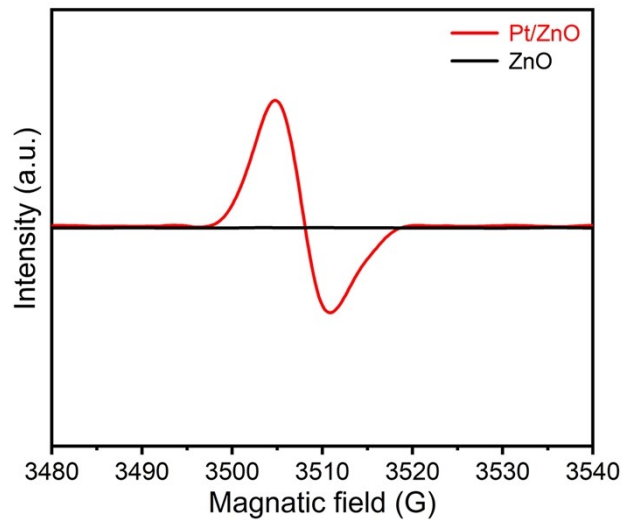


**Fig. S6** EPR spectra of ZnO and Pt/ZnO.



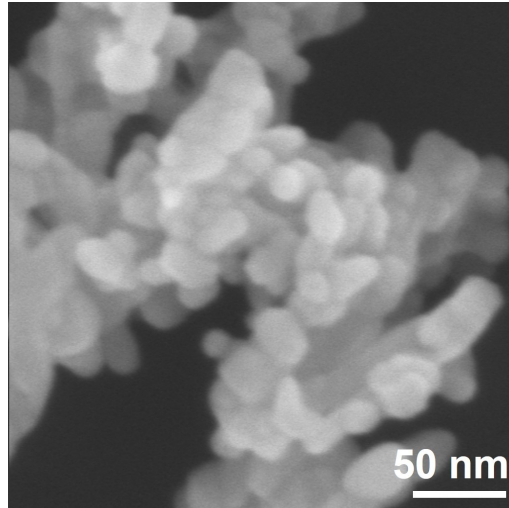


**Fig. S7** FESEM image of pure ZnO.

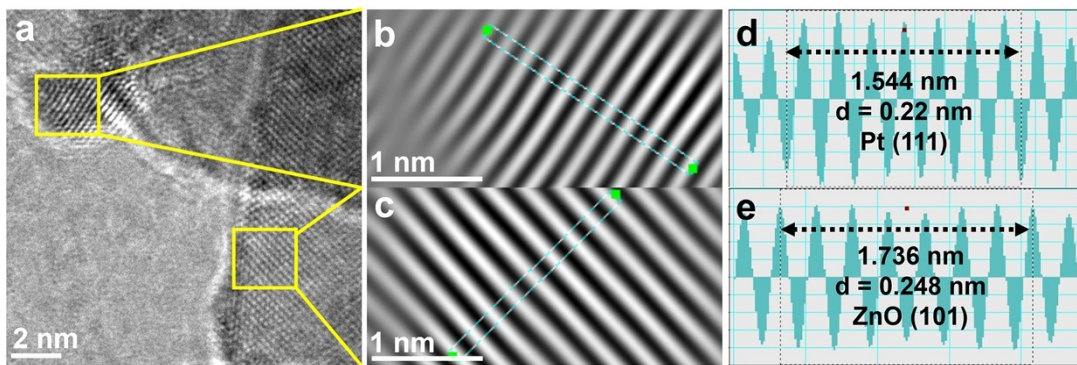


**Fig. S8** (a) HRTEM image, (b,c) the corresponding inverse fast Fourier transform (IFFT) images and (d,e) line scans of Pt/ZnO.

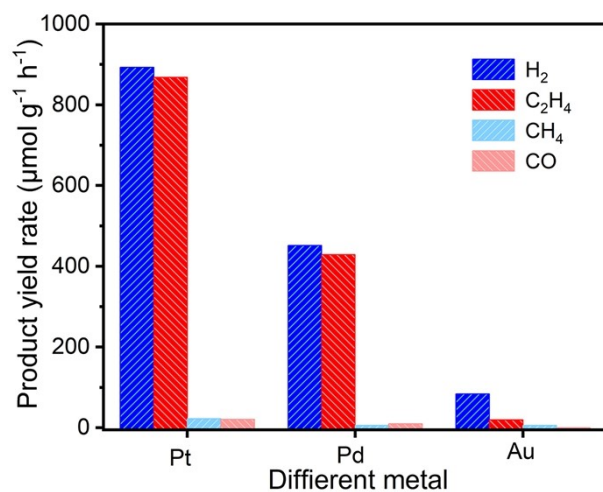


**Fig. S9** Photocatalytic EDH performance of Pt/ZnO, Pd/ZnO and Au/ZnO.

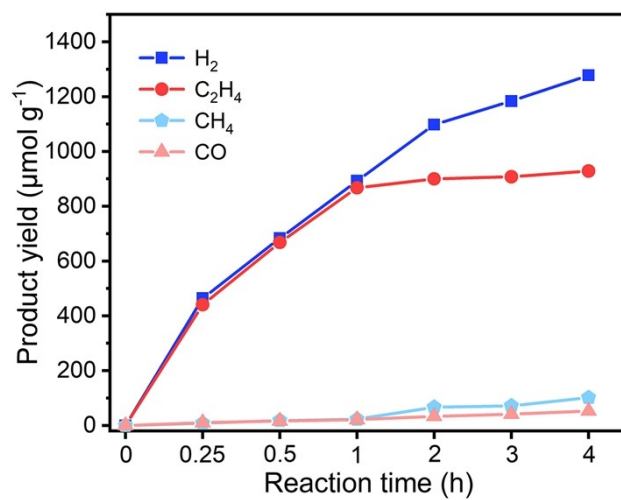


**Fig. S10** Time-yield plots of Pt/ZnO.

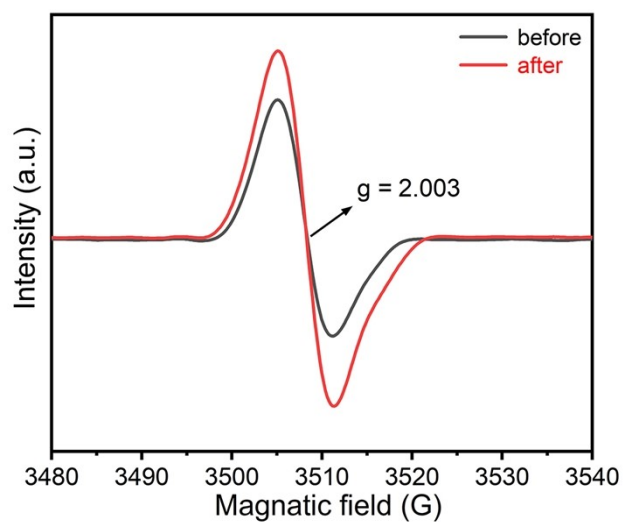


**Fig. S11** EPR spectra of Pt/ZnO samples before and after the EDH reaction.

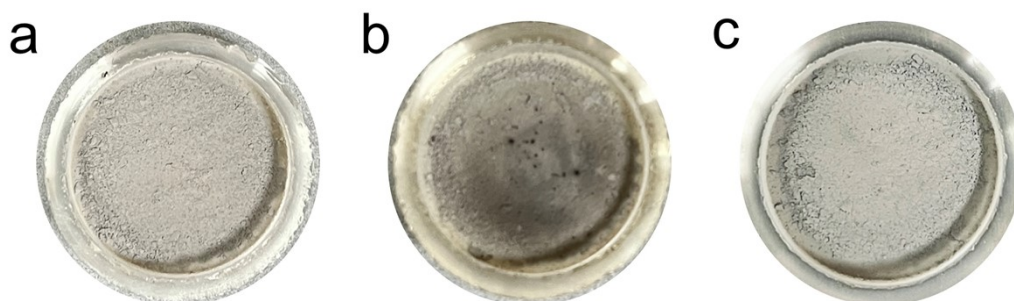


**Fig. S12** Color comparison of Pt/ZnO: (a) fresh sample, (b) used sample after the 6<sup>th</sup> cyclic test and (c) recovered sample.

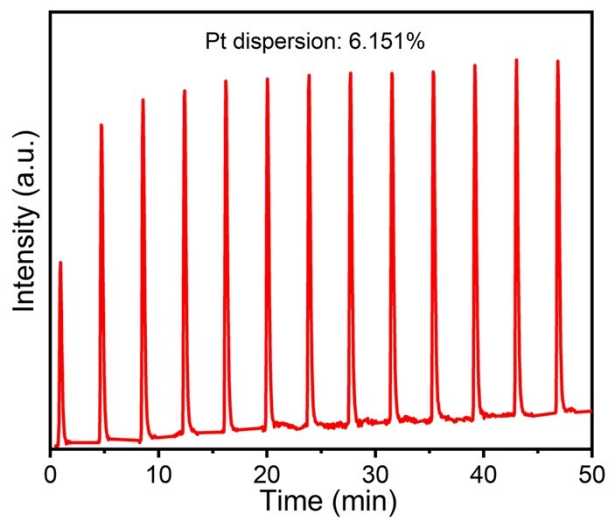


**Fig. S13** CO pulse analysis profile of Pt/ZnO.

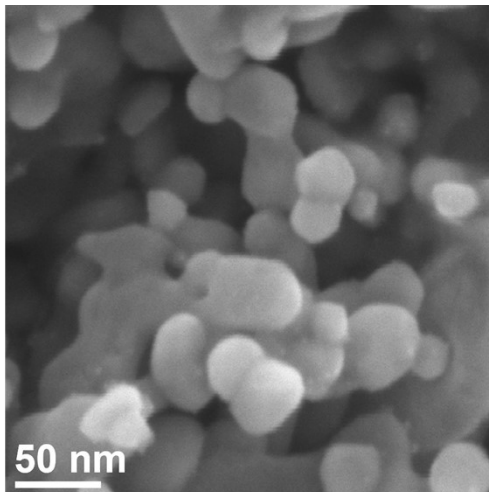


**Figure S14.** FESEM image of spent Pt/ZnO.

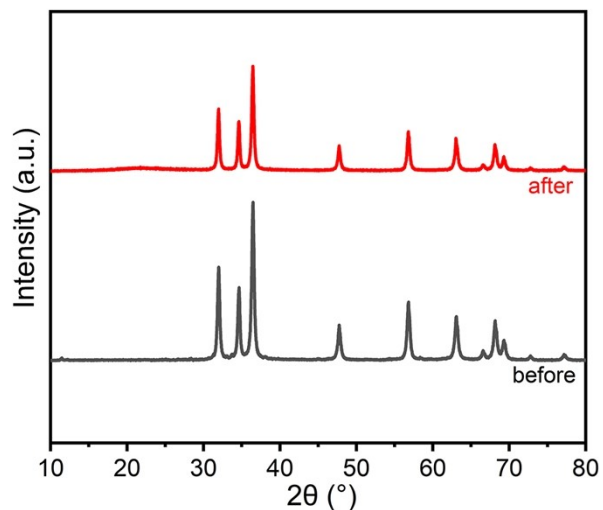


**Fig. S15** XRD patterns of Pt/ZnO before and after eight cyclic tests.

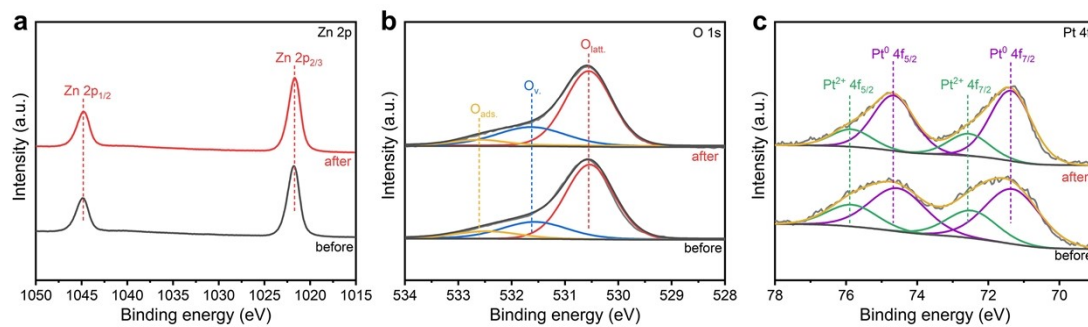


**Fig. S16** (a) Zn 2p, (b) O 1s and (c) Pt 4f XPS spectra of Pt/ZnO before and after eight cyclic tests.

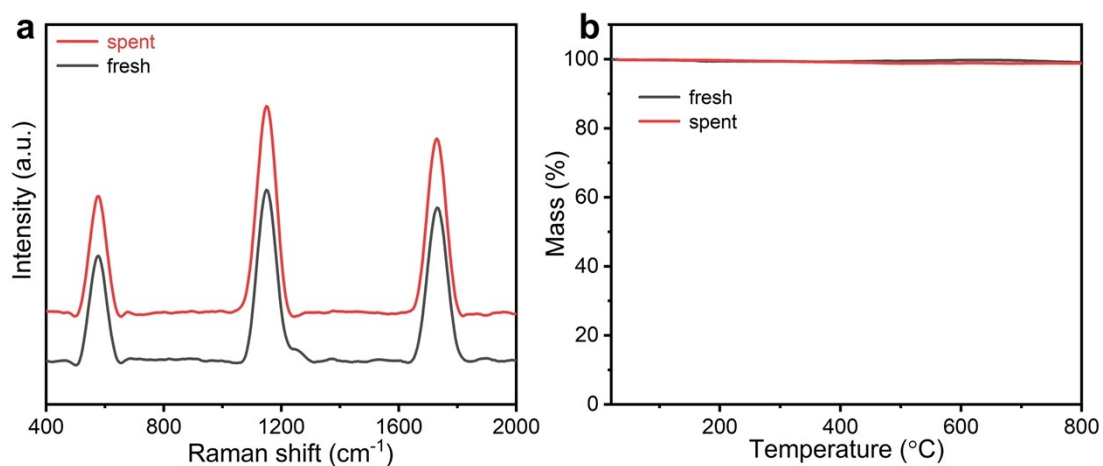


**Fig. S17** (a) Raman spectra and (b) TGA profiles of fresh and spent Pt/ZnO.

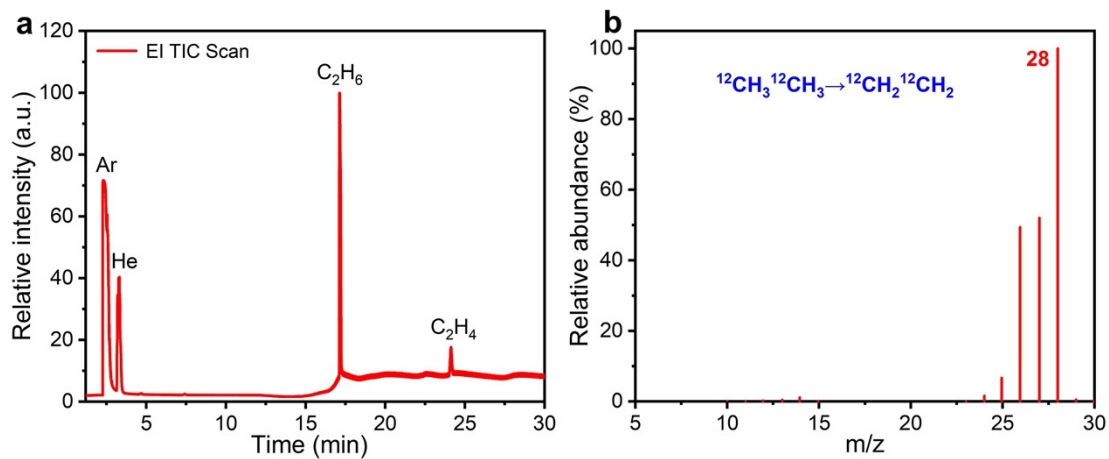


**Fig. S18** The EI TIC scan recorded in GC-MS analysis of (a) ethene using <sup>13</sup>CH<sub>3</sub><sup>12</sup>CH<sub>3</sub> as the feedstock and (b) ethene using <sup>12</sup>CH<sub>3</sub><sup>12</sup>CH<sub>3</sub> as the feedstock.

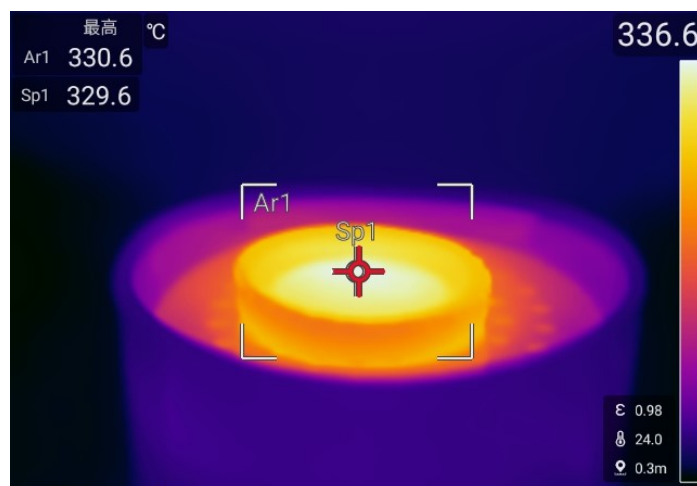


**Fig. S19** The detected catalyst surface temperature of Pt/ZnO during the photocatalytic EDH reaction.

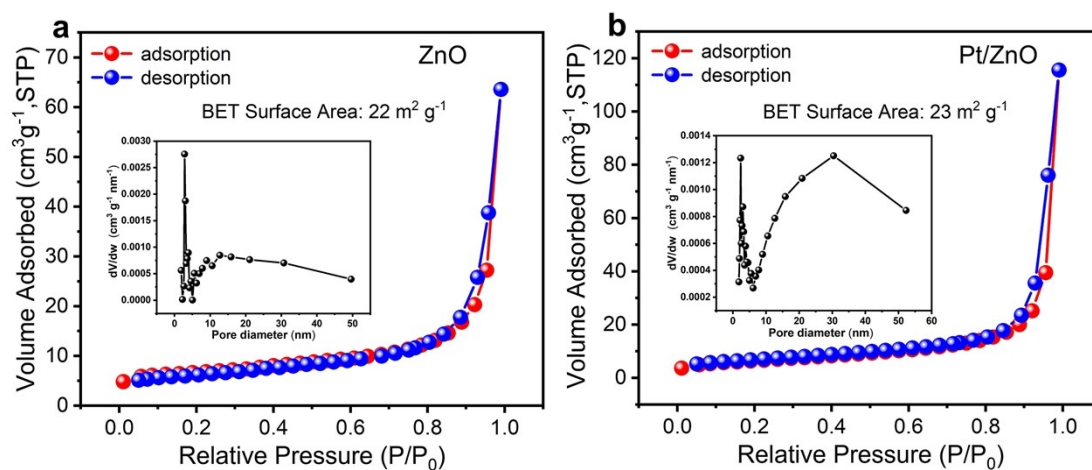


**Fig. S20**  $N_2$  adsorption-desorption isotherms and pore size distribution plots of (a) ZnO and (b) Pt/ZnO.

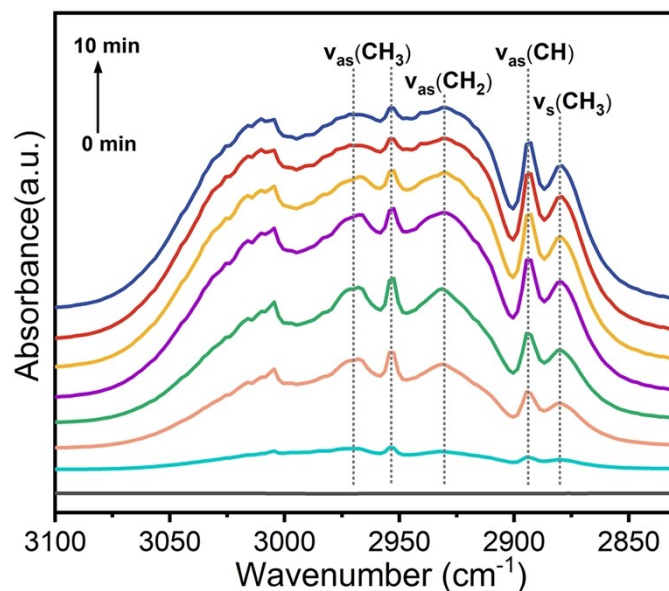


**Fig. S21** *In situ* DRIFTS spectra of adsorbed  $C_2H_6$  on Pt/ZnO at room temperature for different durations.

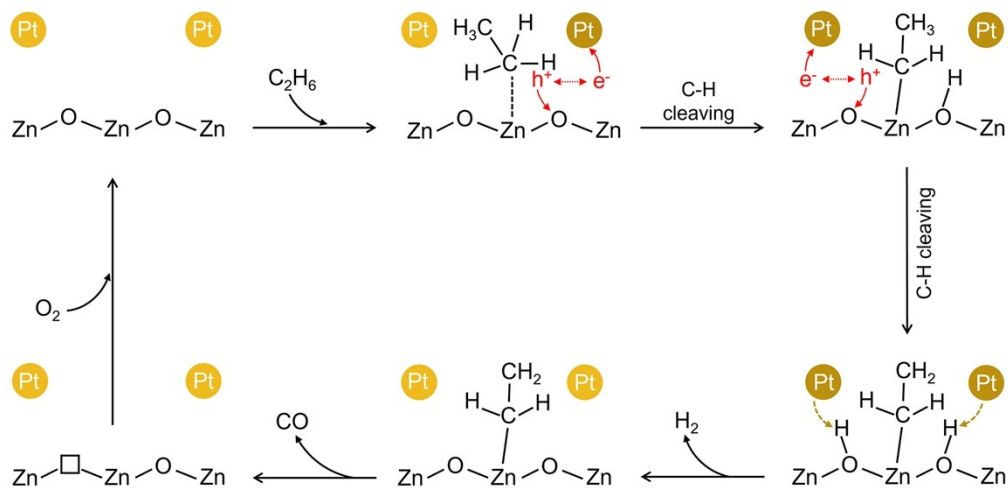


**Fig. S22** The schematic diagram of the proposed photocatalytic EDH process involving  $C_2H_4$  overoxidation to form CO over Pt/ZnO.

**Table S1.** The content of Pt in each sample determined by ICP-OES.

Sample	Pt content (%)
0.2Pt/ZnO	0.17
0.5Pt/ZnO	0.48
1.0Pt/ZnO	0.94
2.0Pt/ZnO	1.76



**Table S2.** Comparison of C<sub>2</sub>H<sub>4</sub> generation rate of Pt/ZnO with those of other catalysts for photocatalytic dehydrogenation of ethane systems

Catalysts	Reaction conductions	C <sub>2</sub> H <sub>4</sub> evolution rate ( $\mu\text{mol h}^{-1} \text{g}^{-1}$ )	Ref.
Pt/ZnO	EDH, C <sub>2</sub> H <sub>6</sub> : Ar = 1: 9, 1 atm batch reaction	867.8	This work
LaVO <sub>4</sub> -O <sub>v</sub>	EDH, undiluted ethane, 1 atm batch reaction	75	1
Cu/TiO <sub>2</sub>	EDH, C <sub>2</sub> H <sub>6</sub> : Ar = 1: 9, 0.2MPa batch reaction	420	2
PdZn-ZnO	EDH with O <sub>2</sub> , C <sub>2</sub> H <sub>6</sub> : O <sub>2</sub> = 5: 1 1 atm, flow reaction	46400	3
Pd/TiO <sub>2</sub>	EDH with CO <sub>2</sub> , C <sub>2</sub> H <sub>6</sub> : CO <sub>2</sub> = 1: 1, 0.2MPa, batch reaction	230.5	4

**Table S3.** Assignments and corresponding vibrational frequencies of the possible species by *in-situ* DRIFTS.

Assignment	Vibrational frequency (cm <sup>-1</sup> )	Possible specie
$\nu$ (OH)	3668, 3473	$\cdot\text{OH}$
$\nu_{\text{as}}$ (CH <sub>3</sub> )	2970, 2953	CH <sub>3</sub> -CH <sub>2</sub> $\cdot$
$\nu_{\text{as}}$ (CH <sub>2</sub> )	2932	$\cdot\text{CH}_2\text{-CH}_2\cdot$
$\nu_{\text{as}}$ (CH)	2894	CH <sub>3</sub> -CH <sub>2</sub> $\cdot$
$\nu_{\text{s}}$ (CH <sub>3</sub> )	2880	CH <sub>3</sub> -CH <sub>2</sub> $\cdot$
$\nu_{\text{as}}$ (C=C)	1552	CH <sub>2</sub> =CH <sub>2</sub>
$\delta_{\text{s}}$ (C=C)	1446	CH <sub>2</sub> =CH <sub>2</sub>
$\delta_{\text{s}}$ (CH <sub>2</sub> )	1408	$\cdot\text{CH}_2\text{-CH}_2\cdot$
$\delta_{\text{s}}$ (CH <sub>3</sub> )	1375	CH <sub>3</sub> -CH <sub>2</sub> $\cdot$
$\nu$ (C-C)	1243, 1063	CH <sub>3</sub> -CH <sub>2</sub> $\cdot$
$\delta_{\text{s}}$ (=CH)	884	CH <sub>2</sub> =CH <sub>2</sub>

Note:  $\delta_{\text{s}}$ : deformation;  $\nu$ : stretching;  $\nu_{\text{s}}$ : symmetrical stretching;  $\nu_{\text{as}}$ : antisymmetric stretching

## Supplementary references

1. F. Wei, W. Xue, Z. Yu, X. F. Lu, S. Wang, W. Lin and X. Wang, *Chin. Chem. Lett.*, 2024, **35**, 108313.
2. L. Song, R. Zhang, C. Zhou, G. Shu, K. Ma and H. Yue, *Chem. Commu.*, 2023, **59**, 478-481.
3. P. Wang, X. Zhang, R. Shi, J. Zhao, G. I. N. Waterhouse, J. Tang and T. Zhang, *Nat. Commun.*, 2024, **15**, 789.
4. R. Zhang, H. Wang, S. Tang, C. Liu, F. Dong, H. Yue and B. Liang, *ACS Catal.*, 2018, **8**, 9280-9286.